Fischer, Michael ; Kim, Won June ; Badawi, Michael ; Lebègue, Sébastien

# Benchmarking the performance of approximate van der Waals methods for the structural and energetic properties of SiO2 and AlPO4 frameworks

Journal Article as: published version (Version of Record)

DOI of this document*(secondary publication): https://doi.org/10.26092/elib/2850

Publication date of this document: 07/03/2024

The Journal of Chemical Physics

# Benchmarking the performance of approximate van der Waals methods for the structural and energetic properties of $SiO_2$ and $AlPO_4$ frameworks

Cite as: J. Chem. Phys. **150**, 094102 (2019); https://doi.org/10.1063/1.5085394
Submitted: 12 December 2018 . Accepted: 08 February 2019 . Published Online: 01 March 2019

Michael Fischer, Won June Kim, Michael Badawi, and Sébastien Lebègue



AIP Publishing

The Journal of Chemical Physics ARTICLE scitation.org/journal/jcp

# Benchmarking the performance of approximate van der Waals methods for the structural and energetic properties of $SiO_2$ and $AlPO_4$ frameworks

Cite as: J. Chem. Phys. 150, 094102 (2019); doi: 10.1063/1.5085394
Submitted: 12 December 2018 • Accepted: 8 February 2019 •
Published Online: 1 March 2019



Michael Fischer,[1,2,a),b)] Won June Kim,[3,a)] Michael Badawi,[3] and Sébastien Lebègue[3]

## AFFILIATIONS

[1]Crystallography Group, Department of Geosciences, University of Bremen, Klagenfurter Straße 2-4, D-28359 Bremen, Germany
[2]MAPEX Center for Materials and Processes, University of Bremen, D-28359 Bremen, Germany
[3]Université de Lorraine and CNRS, LPCT, UMR 7019, 54506 Vandœuvre-lès-Nancy, France

[a)]**Contributions:** M. Fischer and W. J. Kim contributed equally to this work.
[b)]**Electronic mail:** michael.fischer@uni-bremen.de

## ABSTRACT

Density functional theory (DFT) calculations using sixteen different approaches, fourteen of which were designed to include dispersion interactions [DFT + D and van der Waals (vdW)-DF methods], were performed for a set of sixteen framework compounds with either $SiO_2$ or $AlPO_4$ composition. The compounds include four dense structures ($\alpha$-quartz, $\alpha$-cristobalite, and their $AlPO_4$ analogues), eight all-silica zeolites, and four aluminophosphate zeotypes (AlPOs). We analyzed the performance in reproducing the equilibrium structure for all systems, and computed bulk moduli and relative stabilities were compared to experiments for those compounds where experimental data are available. We found that the results obtained with functionals that take into account dispersive interactions are closer to experiments than those obtained with a bare generalized gradient functional. However, the variation among individual methods is considerable, and functionals that perform well for one quantity may give rather large deviations for another. Taking together the whole body of results, it appears that the Perdew-Burke-Ernzerhof functional including a many-body dispersion correction and the rev-vdW-DF2 methods present the best performance for the description of $SiO_2$ and $AlPO_4$ materials.



## I. INTRODUCTION

Conventional density functional theory (DFT) methods are unable to correctly capture dispersion interactions because the long-range electron correlation that is responsible for these interactions is missing when using typical local or semi-local exchange-correlation functionals (such as the local density approximation—LDA or the generalized gradient approximation—GGA). To remedy this shortcoming, a variety of approaches to incorporate van der Waals (vdW) interactions in the framework of DFT have been proposed, which are the subject of several recent review articles.[1–3] While the inclusion of dispersion is pivotal to compute reasonable binding energies for non-covalently bound complexes[4–7] and molecular crystals,[8,9] it also has a significant impact on computations for inorganic materials. In this regard, DFT methods that incorporate van der Waals interactions have been tested—and compared to conventional DFT—for structural, energetic, and (sometimes) other properties for a variety of inorganic systems, among them ionic crystals, simple covalently bonded solids, layered materials, sheet silicates, and several $SiO_2$ polymorphs.[10–14] As a representative example, we briefly summarize the approach and results of Tawfik *et al.*[14] These authors assessed the performance of 11 approximate van der Waals methods for the prediction of interlayer distances $c_0$ and binding energies $E_b$ of several two-dimensional materials like

graphene, boron nitride, and $MoS_2$. Overall, there appeared to be a "trade-off" in the accuracy for structures and energetics: those functionals that gave accurate $E_b$ values typically gave poor interlayer distances and vice versa. Only a few methods, most prominently the Perdew-Burke-Ernzerhof (PBE)-many-body dispersion (MBD)/FI approach, which includes many-body dispersion contributions using a "fractional ion" approach,[15] performed well for both quantities. The authors attributed the shortcomings of other methods to inadequacies in the underlying polarizability models.

Due to their widespread applications in adsorption, ion exchange, and catalysis, zeolites are one group of porous inorganic materials that have attracted the interest of experimentalists and theoreticians alike.[16–19] Approximate van der Waals methods based on DFT have been widely employed to study interactions between guest molecules and zeolite hosts, especially in the context of computational studies of adsorption.[20–26] Moreover, it has been established in the last few years that the inclusion of dispersion interactions is also pivotal to achieve an accurate reproduction of structural properties and thermochemistry of zeolites and related materials. In the following overview, we focus on neutral-framework zeotypes, especially all-silica zeolites, i.e., zeotypes with a pure-$SiO_2$ composition. Before the development of dispersion-corrected DFT, a study by Civalleri *et al.* published in 1998 showed that different exchange-correlation functionals (LDA, GGA-type BLYP, and hybrid B3LYP) all give the same trend in the relative stability of three zeolite frameworks (here, the relative stability is defined with respect to $\alpha$-quartz, the stable $SiO_2$ polymorph at ambient conditions).[27] However, the quantitative variation of the computed energy differences $\Delta E_{DFT}$ (where $E_{DFT}(quartz)$ defines the zero point) was found to be considerable. Astala *et al.* observed that the LDA functional gives rather accurate lattice parameters and Si–O bond distances, whereas the GGA-type PW91 functional overestimates the lattice dimensions and bond lengths.[28] On the other hand, LDA, despite its well-known tendency to "overbind," results in too small $\Delta E_{DFT}$ values when compared to experimental enthalpies of transition $\Delta H_{trans}$. Nevertheless, it is still better than PW91, which gives very small energy differences that sometimes even have the wrong sign, i.e., PW91 predicts some zeolites to be more stable than $\alpha$-quartz. An underestimation of $\Delta E_{DFT}$ that is comparable to that of LDA was also observed for the B3LYP functional, which incorporates a fraction of exact (Hartree-Fock) exchange.[29]

In 2015, two groups of authors showed that the inclusion of dispersion interactions in the DFT calculations greatly improves the accuracy of the calculated structures and properties of all-silica zeolites.[12,30] Studying a total of 14 all-silica zeolites for which experimental enthalpies of transition are available, Román-Román and Zicovich-Wilson showed that use of the hybrid PBE0 functional with a "Grimme-type" dispersion correction (PBE0-D2) results in almost quantitative agreement between the computed $\Delta E_{DFT}$ and experimental $\Delta H_{trans}$ values.[30] They also pointed out that dispersion interactions are to a large extent responsible for the stabilization of $\alpha$-quartz over the less dense zeolitic $SiO_2$ polymorphs. A drawback of the PBE0-D2 functional, however, is the rather poor performance for framework densities (FDs), which are underestimated significantly. Hay *et al.* studied only two zeolites and a few dense $SiO_2$ polymorphs but considered a larger range of DFT approaches that include dispersion.[12] Several of the tested methods [among them PBE-D2, PBE including a dispersion correction devised by Tkatchenko and Scheffler (TS), and vdW-DF2] gave a reasonable prediction of the energy differences as well as rather accurate lattice parameters. However, a closer analysis revealed that the good performance for lattice parameters is due to an error compensation between overestimated Si–O bond distances and underestimated Si–O–Si angles. These findings were essentially corroborated in more recent work by one of us,[31,32] who looked at a larger set of zeolite structures for which accurate crystal structure data are available, including both all-silica zeolites and aluminophosphate zeotypes (AlPOs). In the first of these studies, which included three GGA-type functionals (PBE, PBEsol, and WC) and two dispersion-corrected variants of PBE (PBE-D2 and -TS), the PBE-TS functional came out as the best method, with a mean of absolute errors (MAE) in lattice parameters of 0.052 Å. Since it was found that the PBEsol functional performed much better for T–O bond distances, the second study included two dispersion-corrected variants of this functional, PBEsol-D2 and PBEsol-TS.[32] Both approaches gave very accurate lattice parameters, with MAEs of 0.036 Å and 0.032 Å, respectively, and use of the PBEsol-D2 functional also delivered excellent energetics for all-silica zeolites, with the deviation between $\Delta E_{DFT}$ and $\Delta H_{trans}$ being on the order of the experimental uncertainty of 1 kJ $mol^{-1}$ per formula unit of $SiO_2$. In a very recent study, Albavera-Mata *et al.* covered a larger range of exchange-correlation functionals, including revised versions of PBE and RPBE dubbed lsPBE/lsRPBE, respectively, as well as related hybrid functionals.[33] Moreover, the authors used a Grimme-type dispersion correction, deriving a bespoke scaling factor $s_6$ for each functional on the basis of molecular reference data. The performance of the different "families" of functionals was then assessed by comparing the predicted relative stabilities and molar volumes of $SiO_2$-zeolites to experimental reference data. While the best functional, lsRPBE-D, gave rather good agreement for energetics (MAE of 1.9 kJ $mol^{-1}$ per $SiO_2$ unit), an overestimation of the molar volume (=underestimation of framework density) remained prominent.

The present study builds on previous studies on neutral-framework zeotypes that evaluated the accuracy of DFT calculations in reproducing crystal structures and relative stabilities.[31,32] However, it greatly expands the range of approaches studied: in addition to the PBE-D2 and PBE-TS methods, newer variants of the pairwise "Grimme-type" dispersion correction and TS-based many-body dispersion schemes were included, as well as several members of the non-local vdW-DF family of methods. We limit the investigation to approaches that calculate the exchange-correlation energy on the GGA level of theory, as these functionals are currently of most practical relevance to studies of zeolite structures, properties, and dynamics. Besides considering a much larger number of approaches, this study also goes beyond previous work by including bulk moduli as an additional quantity that is used in

the benchmarking. In the following, we first give an overview of the different methods considered and summarize the reference data used to benchmark the calculations. We then analyze the average deviations between DFT and experiments for lattice parameters, T–O bond distances, and T–O–T angles for the whole set structures, before presenting an assessment of the performance for bulk moduli and for energetics, considering only those systems where experimental data are available.

## II. COMPUTATIONAL METHODS

### A. Nonlocal van der Waals density functionals (vdW-DFs)

For the family of nonlocal vdW-DF functionals,[34] the exchange-correlation functional is written as the sum of the GGA exchange, the LDA correlation, and a non-local correlation functional, which is defined as

$$E_c^{nl}[n] = \frac{1}{2}\iint d^3r d^3r' n(\mathbf{r})\phi(\mathbf{r},\mathbf{r}')n(\mathbf{r}'), \quad (1)$$

where $n(\mathbf{r})$ is the electron density at the point $\mathbf{r}$ and $\phi(\mathbf{r}, \mathbf{r}')$ is a non-local kernel that is approximated by a plasmon-pole model. The variants of vdW-DF functionals have been designed by choosing different GGA exchange functionals or different gradient expansions in the non-local kernel to reproduce various asymptotic behaviors of exchange-correlation energy. The original vdW-DF1 of Dion *et al.* used the revPBE exchange functional and $Z_{ab} = -0.8491$ for the coefficient of the gradient expansion in the kernel.[34–36] In the second version, named vdW-DF2,[37] the original GGA exchange is replaced with the less repulsive PW86 exchange,[38] and by setting $Z_{ab} = -1.887$, a more accurate description for atoms and molecules is obtained.

In the last ten years, these functionals have been further improved by modifying the exchange part. Starting from vdW-DF1 functional, Klimeš *et al.* proposed three new functionals, optPBE-vdW, optB88-vdW, and optB86b-vdW, obtained by reparameterizing the PBE, B88, and B86b exchange functional, respectively.[39,40] More recently, Berland and Hyldgaard designed a new exchange functional, LV-PW86r, which is consistent with the nonlocal correlation of vdW-DF1, and therefore proposed the vdW-DF-cx functional, where cx stands for *consistent exchange*.[41] Meanwhile, Hamada improved the vdW-DF2 functional by replacing the PW86 exchange functional with the B86R functional,[42] resulting in the rev-vdW-DF2 functional.[43]

### B. Dispersion correction methods (DFT + D)

The DFT + D methods add *a posteriori* a correction for the dispersion energy on top of the DFT total energy. In the first generation of these methods, the dispersion energy was written as a sum of pairwise terms ($-C_{6,AB}/R_{AB}^6$), multiplied by a damping function to cut out the divergence at small distance: Grimme's D2,[44] D3,[45,46] and Tkatchenko-Scheffler (TS)[47] methods are well-known schemes in this category and they differ by the way employed to calculate the coefficients $C_{6,AB}$ and the vdW radii. The D2 method uses the coefficients of isolated atoms so that the coefficients do not depend on the chemical situation of the atom in the molecular/solid system.[44] The D3 method, on the contrary, adjusts the vdW coefficients of an atom on the basis of the coordination number around the atom.[45,46] In the TS method,[47] the $C_6$ coefficients, vdW radii, and atomic polarizabilities of the atoms in the molecule or in the solid are scaled from those of free atoms, by calculating the ratio between the volume occupied by an atom in his environment $V^{eff}$ and the free non-interacting reference $V^{free}$ using Hirshfeld partitioning. An improvement of the TS method was achieved by considering the ionic state of the atoms through the iterative Hirshfeld scheme,[48] leading to the TS/HI method.[49]

Then the original TS scheme was improved several times to describe the many-body nature of the dispersion interaction, which is not included in the pairwise methods. The first improvement was done by including the long-range electrostatic screening: in this new scheme, which is called the Tkatchenko-Scheffler + self-consistent screening (TS + SCS) method, Dyson-like SCS equations are solved to get screened atomic polarizabilities.[50] However, the many-body dispersion interaction energy, which is important for solids or macromolecular systems, is still not completely captured by the TS + SCS method.[51] The many-body dispersion (MBD) scheme proposed to model the remaining part of the interaction as a set of quantum harmonic oscillators (QHOs) coupled through a dipole-dipole potential.[50] Especially, it has been shown[52] that the energy difference between the coupled system and the uncoupled system of QHOs is equal to the RPA energy of this model system and is written as

$$E_{disp} = \int_0^\infty \frac{d\omega}{2\pi} \ln\det\left[C^{RPA}(i\omega)\right], \quad (2)$$

in which the $C^{RPA}$ matrix is defined as

$$C^{RPA}(i\omega) = \delta_{pq} + (1-\delta_{pq})\alpha_p(i\omega)\tau_{pq}, \quad (3)$$

where $\tau_{pq}$ is the dipole-dipole interaction tensor and $\alpha_p(i\omega)$ is the atomic polarizability. In practice, a range separation scheme is introduced in the dipole-dipole interaction tensor so that Eq. (2) is further modified to couple the SCS and MBD approaches, an approach known as the MBD@rsSCS method.[52] Recently, Gould *et al.* proposed two refinements of the MBD@rsSCS scheme, which is named MBD@rsSCS/FI.[15] First, they have used the gas phase polarizability of fractional ions[53] as the reference of the volume scaling to fully take into account the possible ionic nature of the system. Second, they introduced an "eigenvalue remapping" method to avoid unphysical polarization catastrophes during the calculation.[15] As a short-hand notation that reflects the use of the PBE exchange-correlation functional with these methods, we employ the abbreviations PBE-MBD and PBE-MBD/FI to designate the MBD@rsSCS and MBD@rsSCS/FI methods throughout the remainder of this article.

### C. Computational details

The calculations presented in this work have been performed using the VASP (Vienna *ab initio* simulation package) code.[54,55] We have used the default VASP projector augmented wave (PAW) potentials of version 5.2 with four valence electrons for Si ($3s^2 3s^2$), three for Al ($3s^2 3p^1$), five for P ($3s^2 3p^3$), and six for O ($2s^2 2p^4$). For each system and with each functional, we optimized the structures by following a procedure to remove as much as possible the Pulay stress. First, we fitted the energy-volume curve to a Vinet equation of the state[56]

$$E(\eta) = E_0 + \frac{2K_0V_0}{(K_0' - 1)^2}\{2 - [5 + 3K_0'(\eta - 1) - 3\eta]e^{-3(K_0'-1)(\eta-1)/2}\}, \quad (4)$$

where $\eta = (V/V_0)^{1/3}$. From this, the equilibrium volume $V_0$ and the bulk modulus $K_0$ of each system are obtained. Then, we obtained our fully relaxed structure by reoptimizing it using the fitted volume, $V_0$, obtained from the previous step. To reduce the noise in the energy-volume curve, we have used a kinetic energy cutoff of 500 eV for the plane-wave basis and Γ-centered k-meshes with a grid size of 0.4 $Å^{-1}$. The electronic iterations were continued until the total energy difference between successive steps became smaller than $10^{-6}$ eV. The geometry optimizations were performed until the maximum value of each component of the atomic forces was smaller than 0.01 eV $Å^{-1}$. In the calculations using the TS method and its variants, the exchange-correlation energy was obtained using the Perdew-Burke-Ernzerhof (PBE) functional.[35] A detailed discussion of the TS and MBD implementations in the VASP code can be found in previous publications[15,57,58] and will not be repeated here. Calculations using the non-local vdW functionals, vdW-DF2 and rev-vdW-DF2 calculations, were performed using the implementation provided in VASP.[37,39,40,59] VASP was also used for the vdW-DF-cx functional with the implementation of Björkman.[60]

## III. REFERENCE DATA AND ERROR ANALYSIS

### A. Reference data—Structures

DFT calculations were performed for a total of 16 different structures with a neutral framework and either $SiO_2$ or $AlPO_4$ composition. This set of reference structures consists of four dense structures, namely, α-quartz and α-cristobalite as well as their $AlPO_4$ analogues, eight all-silica zeolites, and four aluminophosphate zeotypes. All structures as well as the references from which the experimental crystal structure data were taken are compiled in Table I. In the following, all-silica zeolites will be typically referred to by their framework type code (FTC) alone,[61] whereas the subscript "AlPO" is added to the FTC for aluminophosphate zeotypes.

The selection of suitable reference structures follows the guidelines outlined in more detail in Ref. 31. For example, only crystal structures determined at room temperature or lower temperatures were included in the reference set, and zeolite/zeotype structures were considered only when the structure determination had been performed for a calcined sample.

**TABLE I.** Overview of structures.

| Topology | Name or acronym | References |
|---|---|---|
| $SiO_2$ systems | | |
| qtz[a,b] | α-quartz | 62 |
| crs[a,b] | α-cristobalite | 63 |
| CHA[a] | $SiO_2$-chabazite | 64 |
| FAU[a,b] | Dealuminated zeolite Y | 65 |
| FER[a,b] | $SiO_2$-ferrierite | 66 |
| IFR[a] | ITQ-4 | 67 |
| LTA | ITQ-29 | 68 |
| RTE | RUB-3 | 69 |
| SAS | SSZ-73 | 70 |
| TON[b] | ZSM-22 | 71 |
| $AlPO_4$ systems | | |
| qtz[b] | α-berlinite | 72 |
| crs | Cristobalite-type $AlPO_4$ (LT form) | 73 |
| AEN | AlPO-53(B) | 74 |
| CHA | AlPO-34 | 75 |
| ERI[b] | AlPO-17 | 76 |
| EZT | EMM-3 | 77 |

[a]Experimental $\Delta H_{trans}$ available.
[b]Experimental $K_0$ available.

### B. Reference data—Bulk moduli

Experimental values of the bulk modulus $K_0$ are available only for a subset of systems, namely, α-quartz,[78] α-cristobalite,[79] α-berlinite,[80] $SiO_2$ zeolites with FAU,[81] FER,[82] and TON topologies,[83] and for AlPO-17 ($ERI_{AlPO}$).[84] For the majority of systems where bulk moduli from more than one source are available, these agree very well with each other, an exception being α-cristobalite, where values between 11.5 and 18 GPa have been reported. Here, an intermediate value of 16.4 GPa obtained from Brillouin spectroscopy experiments was taken as reference value.[79]

### C. Reference data—Energies

Finally, the performance of the different methods in predicting the enthalpies of transition of all-silica zeolites and α-cristobalite with respect to α-quartz was assessed. In a first approximation, the enthalpy of transition $\Delta H_{trans}$ was approximated with $\Delta E_{DFT}$, the difference in DFT energy (per $SiO_2$ unit) between a given $SiO_2$ polymorph and α-quartz, following previous studies.[30,32] Since experimental enthalpies of transition have been measured for a collection of zeolites that differs considerably from the set of reference structures described above, a direct point-by-point comparison is possible only for a subset of frameworks from Table I for which experimental $\Delta H_{trans}$ values are available (α-cristobalite, CHA, FAU, FER, and IFR). An alternative, qualitative possibility to analyze the results arises from the well-known correlation between the framework density (FD) and the enthalpy of transition.[85,86] Consequently, it can be evaluated how closely the $\Delta E_{DFT}$ values obtained with different functionals fall to a trendline calculated on the basis of available experimental $\Delta H_{trans}$ values. This trendline was represented by the following equation:

$$\Delta H_{trans} = 1.022\,58(26.52 - FD). \quad (5)$$

Here, $FD$ is the framework density in T atoms per 1000 Å$^3$, and the resulting $\Delta H_{trans}$ is in kJ mol$^{-1}$. The equation was set up in a way that it gives an enthalpy of zero for the framework density of $\alpha$-quartz. A comparison of experimental $\Delta H_{trans}$ values to those calculated from this equation is supplied in the supplementary material. The deviations between calculated and experimental values are on the order of the typical experimental error of 1 kJ mol$^{-1}$, indicating that this correlation should serve as a suitable reference to gauge the performance of various DFT methods in terms of energetics.

### D. Assessment of errors

With regard to structural parameters, the agreement between a DFT-optimized structure and the experimental reference was analyzed in terms of lattice parameters, framework densities $FD$ (where $FD = 1000 \cdot \frac{N_T}{V_{uc}}$, with $N_T$ being the number of T atoms per unit cell and $V_{uc}$ the unit cell volume) as well as T–O bond distances and T–O–T angles. In each case, the error in a given quantity $x$ between DFT calculation and experiments was calculated as

$$err_x = x_{DFT} - x_{exp}. \quad (6)$$

Errors in bulk modulus were calculated according to Eq. (6) for six systems for which experimental bulk moduli have been determined, excluding $ERI_{AlPO}$ for reasons discussed below. For the relative stability with respect to $\alpha$-quartz, $err_x$ was calculated as the difference between the DFT energy difference $\Delta E_{DFT}$ and the experimental enthalpy of transition $\Delta H_{trans}$, and including only those five $SiO_2$ systems where experimental values are available.

In order to calculate the overall error in a given quantity from the individual errors $err_x$, the mean of absolute errors (MAE, also termed the mean of unsigned errors MUE by many authors) was calculated as

$$\mathrm{MAE} = \frac{1}{N_i}\sum_{i=1}^{N_i}\left|err_{x,i}\right|. \quad (7)$$

While the MAE is a useful measure of the overall deviation, it does not give insights into systematic over- or underestimations. Such systematic errors can be identified by analysing the mean of signed errors (MSE)

$$\mathrm{MSE} = \frac{1}{N_i}\sum_{i=1}^{N_i} err_{x,i}. \quad (8)$$

## IV. RESULTS AND DISCUSSION

### A. Structural parameters

#### 1. Lattice parameters and framework densities

The mean of signed errors and mean of absolute errors in lattice parameters obtained with the different functionals are shown in Fig. 1 (numerical values are tabulated in the supplementary material). Prior to discussing the performance of the different approaches, we note in passing that the MAE and MSE values obtained with the PBE, PBEsol, PBE-D2, and PBE-TS functionals are slightly larger than the corresponding errors computed in a previous benchmarking study on an almost identical set of reference structures, which used the CASTEP code with on-the-fly generated ultrasoft pseudopotentials.[31] However, as a comparison between different codes is not the aim of the present study, we do not attempt to elucidate these differences and focus exclusively on the results obtained with VASP and projector-augmented waves.

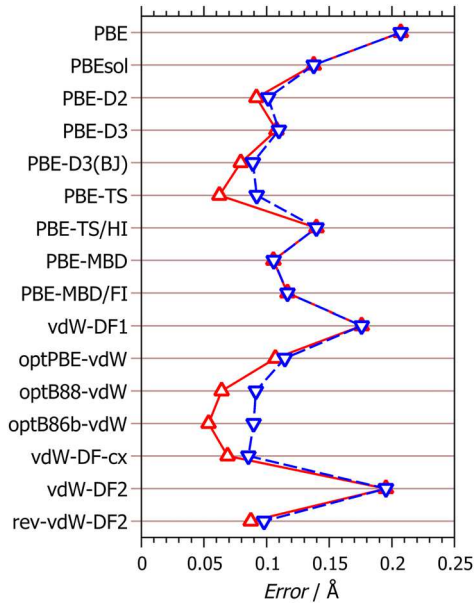


**FIG. 1**. Mean of signed errors (red upright triangles) and mean of absolute errors (blue inverse triangles) in lattice parameters.

When comparing the performance of the different functionals implemented within VASP, it is apparent that the GGA-type functionals, PBE and PBEsol, systematically overestimate the lattice parameters. While the considerable error of PBE (MAE = 0.207 Å) is reduced by about one third when replacing it by PBEsol, the fact that MAE and MSE are equal even for the latter functional shows that all individual lattice parameters are overpredicted. The three variants of PBE with a Grimme-type dispersion correction exhibit a rather similar behavior, all of them performing better than PBEsol, but also overestimating the lattice dimensions. The best choice of the three appears to be the PBE-D3(BJ) functional. The original PBE-TS functional gives an MAE of a similar magnitude to PBE-D3(BJ), but a smaller MSE. Interestingly, use of the TS/HI correction scheme significantly worsens agreement between DFT and experiments. PBE-MBD and -MBD/FI are better than PBE-TS/HI, but worse than PBE-TS, and overpredict all lattice parameters (MSE = MAE).

Moving to the vdW-DF family of approximations, we find that vdW-DF1 and vdW-DF2 perform almost as badly as PBE, despite the inclusion of dispersion interactions (as we will see

below, this is at least partly related to a considerable overestimation of the T–O bond lengths). The other five functionals all provide decent agreement, with MAEs in the range of 0.10 Å, with optB88-vdW, optB86b-vdW, and vdW-DF-cx giving somewhat smaller errors than optPBE-vdW and rev-vdW-DF2. Moreover, their use results in relatively small MSEs between 0.05 and 0.07 Å, i.e., these functionals have a less pronounced tendency to overestimate the lattice parameters. They are essentially on par with PBE-TS.

Since most of the experimental crystal structures were refined from data obtained at room temperature, there is a systematic difference between DFT values—which correspond to the equilibrium lattice dimensions at 0 K—and the experimental values. We have shown in a previous study for the case of the PBEsol-D2 and PBEsol-TS functionals that the use of low-temperature, rather than room-temperature experimental data as reference tends to improve agreement between DFT and experiments (such low-temperature data are available only for a few structures from the reference set).[32] However, the observed changes in MSE and MAE values were fairly small, on the order of 0.01–0.015 Å. Since the MAEs and MSEs found above are significantly larger than this difference, and since all functionals show a similar tendency to overestimate the lattice dimensions, an inclusion of the effect of temperature on the lattice parameters would not alter the qualitative findings regarding the more and less accurate functionals.

Before moving towards bond lengths and angles, we take a look at the framework densities, where the overall errors are shown in Fig. 2. All MSEs are negative, meaning that all functionals underestimate the framework density, a consequence of the general tendency to overestimate the lattice dimensions found above. PBE-TS, optB88-vdW, and optB86b-vdW underestimate *FD* only modestly, with MSEs between −0.13 and −0.18 T atoms per 1000 Å$^3$ (the absolute magnitude of the framework densities ranges from about 13 to 26 T atoms per 1000 Å$^3$, so these errors are on the order of one per cent). With regard to the absolute error, there are several "good" functionals with MAE values between 0.3 and 0.4 T atoms per 1000 Å$^3$, namely, PBE-D2, PBE-D3(BJ), PBE-TS, optB88-vdW, optB86b-vdW, vdW-DF-cx, and rev-vdW-DF2. Unsurprisingly given the previous findings, PBE, vdW-DF1, and vdW-DF2 perform worst.

### 2. T–O bond lengths

Since the T–O bond lengths for a given species of T scatter around an equilibrium value, it is insightful to calculate the average T–O bond distances $d_{aver}$, considering all non-equivalent bonds in the different structures. The average T–O bond distances, including standard deviations, are shown in Fig. 3. For a given DFT approach, the MSE is, by definition, equal to the difference between the experimental $d_{aver}$ and the DFT value; therefore, the MSEs are not shown separately. However, the mean of absolute errors in the T–O distances are included in Fig. 4.

First of all, we may note that PBE overestimates the T–O bond lengths significantly, with the differences in the average bond distance ranging from 0.01 Å for P–O bonds to 0.03 Å for Al–O bonds (MAEs between 0.019 and 0.029 Å). Most dispersion-corrected PBE-based approaches give only minimally shorter equilibrium bond distances than PBE, and the MAEs are also similar. A notable exception is the PBE-MBD

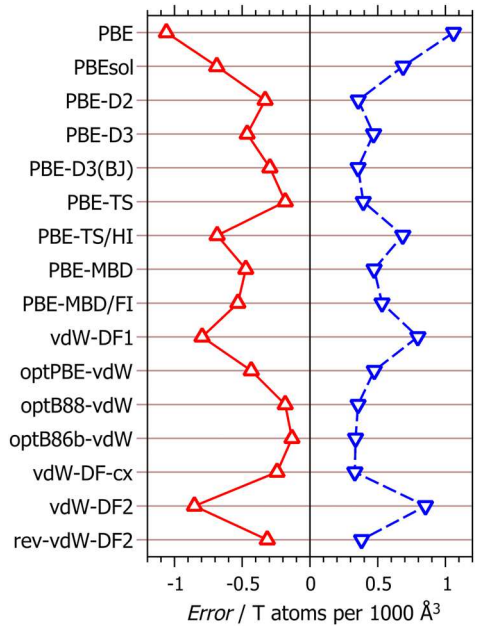


**FIG. 2**. MSE (red upright triangles) and MAE (blue inverse triangles) in framework densities.

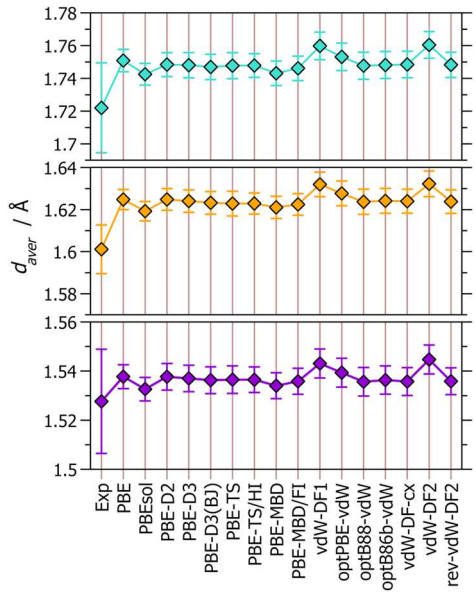


**FIG. 3**. Average Si–O (orange), Al–O (turquoise), and P–O (purple) bond lengths. Error bars indicate the standard deviations from the average value.

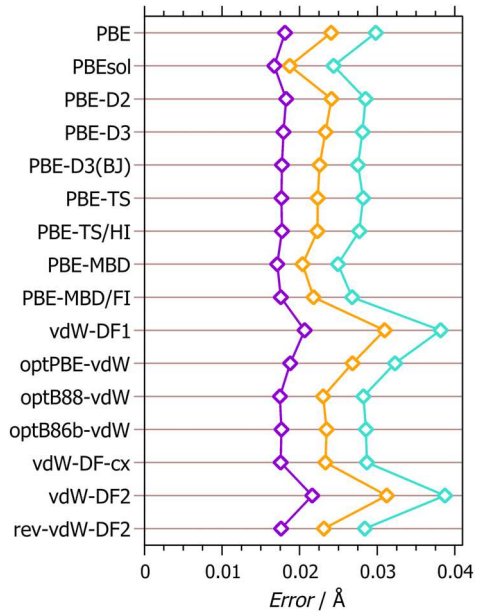


**FIG. 4**. MAE in Si–O (orange), Al–O (turquoise), and P–O (purple) bond lengths.

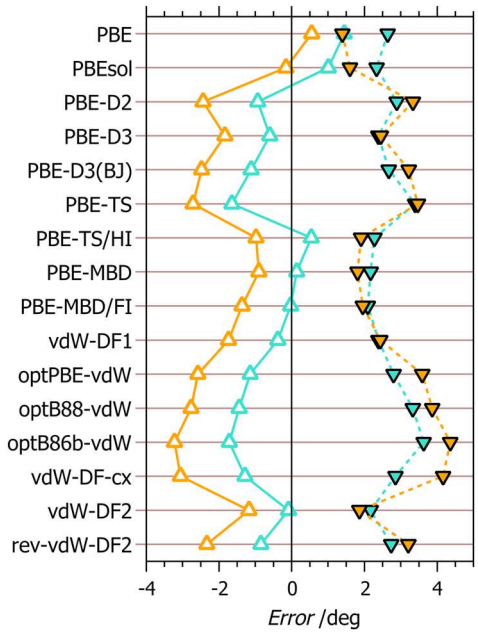


**FIG. 5**. MSE (upright triangles) and MAE (inverse triangles) in Si–O–Si (orange) and Al–O–P (turquoise) angles.

functional, which—like PBEsol without dispersion correction—results in shorter bond lengths and therefore smaller MAEs for Si–O and Al–O bonds. Among the vdW-DF approximations, the vdW-DF1, optPBE-vdW, and vdW-DF2 functionals result in an even stronger overestimation of T–O bond distances than PBE, whereas optB88-vdW, optB86b-vdW, vdW-DF-cx, and rev-vdW-DF2 are on par with PBE and its derivatives.

As a final remark with regard to the bond lengths, we have to note that, in framework compounds, thermal vibrations lead to a shortening of the "apparent" (observed) T–O bond lengths in comparison to the actual values. For structures determined at room temperature, the magnitude of this shortening is on the order of 0.005 Å.[87] Correcting the experimental bond lengths to account for this effect (as we have done for a subset of structures in a previous study[32]) would improve the overall agreement between DFT and experiments; however, significant deviations would remain.

### 3. T–O–T bond angles

As the last structural parameter, we compare the T–O–T angles delivered by the DFT computations to experimental values. Unlike O–T–O angles, which remain close to the tetrahedral angle due to the rigidity of the $TO_4$ tetrahedra, the T–O–T angles show a rather large variation: In the set of experimental reference structures, the observed Si–O–Si angles range from 138.4° to 167.4° and Al–O–P angles cover an even larger range from 132.2° to 173.2°.

The MAE and MSE values for Si–O–Si and Al–O–P bond angles are shown in Fig. 5. For Si–O–Si angles, the functionals without dispersion correction, PBE and PBEsol, give no systematic under- or overestimation (MSE close to zero) and small MAEs of roughly 1.5°. Among the dispersion-corrected approaches, the sophisticated PBE-based approaches PBE-TS/HI, -MBD, and -MBD/FI as well as vdW-DF2 also deliver reasonable agreement with experiments, with MAEs below 2° and only a weak tendency to underestimate the Si–O–Si angle. The PBE-D3 and vdW-DF1 functionals form a third group, with MAEs of about 2.5°, whereas all other DFT + D and vdW-DF approaches perform significantly worse. The negative MSE values of these functionals, which mostly fall between −2° and −3°, indicate a systematic underestimation of the Si–O–Si angles, in accordance with earlier studies.[12,31,32] As discussed previously, such an underestimation is likely related to an overestimation of the dispersive interaction between the two T atoms at opposite sides of the T–O–T linkage, which favours smaller T–T distances and therefore smaller T–O–T angles. The trends in the overall errors for Al–O–P angles are altogether similar to those found above, with PBE-TS/HI, -MBD, -MBD/FI, and vdW-DF2 giving the smallest MAEs. Interestingly, these functionals also have no systematic tendency to underestimate the Al–O–P angles, with MSEs that are essentially zero.

## B. Bulk moduli

The MSE and MAE in bulk moduli were calculated on the basis of datapoints for six of the seven systems for which experimental values are available, omitting $ERI_{AlPO}$ for reasons explained below. The calculated errors are shown in Fig. 6. Since the experimental values range from 18 to 38 GPa, MAEs on the order of 3 GPa correspond—roughly—to relative errors on the order of 10%–15%. PBE and PBEsol as well as PBE-TS, vdW-DF1, and vdW-DF2 give large MAEs above 4.5 GPa, with the three latter functionals showing a systematic

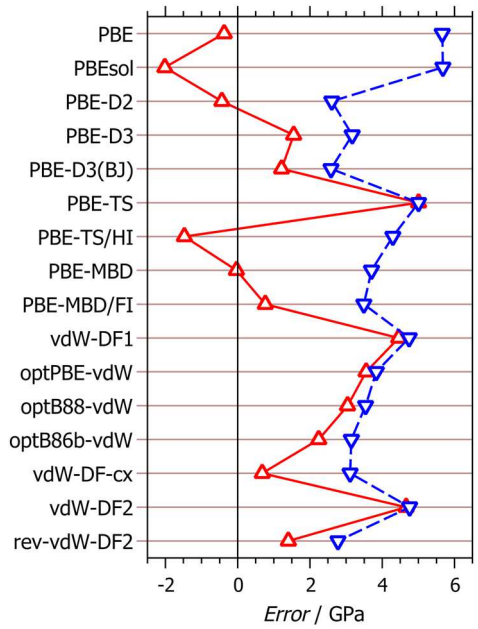


**FIG. 6**. MSE (red upright triangles) and MAE (blue inverse triangles) in bulk moduli.

tendency to overestimate the bulk modulus. The considerable deviations observed for PBE-TS are quite surprising, as this method was found to give a rather accurate prediction of $K_0$ for a template-containing fluoroaluminophosphate zeotype in a recent computational study.[88] The best results are obtained with the PBE-D2, PBE-D3(BJ), and rev-vdW-DF2 functionals, with MAEs on the order of 2.5 GPa, whereas all other functionals give MAEs between 3 and 4.5 GPa.

The experimental value of $K_0$ for $ERI_{AlPO}$ (AlPO-17), which was obtained from the evolution of the unit cell volume upon compression up to pressures of 1.3 GPa, amounts to 31.2 GPa.[84] Interestingly, the compressibility increases with pressure, an unusual behavior that points to an elastic instability. The peculiar elastic properties of AlPO-17 are also evidenced by its pronounced negative thermal expansion.[76] The DFT calculations deliver bulk moduli between 47 and 64 GPa, values that are 50%–100% larger than the experimental $K_0$. As such drastic deviations are observed regardless of the choice of functional, we must assume that there is a fundamental problem for this particular system. Although we have confidence in the computational results, we cannot determine the reason for the disagreement between theory and experiments at this point. In any case, the inclusion of $ERI_{AlPO}$ in the calculation of MSE and MAE would affect the resulting values to an extent that the overall performance of a given functional would be obscured. Therefore, it was omitted from the overall error calculation.

### C. Relative stability of $SiO_2$ systems

The full set of computed $\Delta E_{DFT}$ values obtained for $SiO_2$ systems with different functionals is given in the supplementary material. In the analysis presented here, we look at two different aspects: first, we classify the functionals according to the MSE and MAE values calculated for the subset of structures for which experimental enthalpies of transition are available ($\alpha$-cristobalite, CHA, FAU, FER, and IFR). Following this, we illustrate the performance of some representative functionals by plotting the $\Delta E_{DFT}$ values against the trendline based on experimental data. We omit the pure-GGA functionals PBE and PBEsol from the discussion because these functionals give values of $\Delta E_{DFT}$ that are close to zero (sometimes even negative), regardless of the framework density, thus failing to reproduce even the general trend of increasing $\Delta E_{DFT}$ with decreasing *FD*. This behavior has been observed in previous studies and is only corroborated here.[12,31]

The MAE and MSE values of the approximate van der Waals methods are shown in Fig. 7. According to the overall errors, we may group the functionals as follows:

- **MAE > 2 kJ mol$^{-1}$, MSE negative:** These functionals deliver too small energy differences, i.e., they underestimate the relative instability of the less dense $SiO_2$ polymorphs with respect to $\alpha$-quartz. This is the case for the PBE-TS/HI and PBE-MBD/FI functionals.
- **MAE < 2 kJ mol$^{-1}$:** These functionals give a fairly reasonable prediction of the relative stabilities. Among the six functionals falling in this category, PBE-D2, PBE-D3, and PBE-MBD all have MAE values of 1 kJ mol$^{-1}$ or less, thus being significantly better than the other three, PBE-D3(BJ), vdW-DF2, and rev-vdW-DF2, for which the MAEs are between 1.5 and 2 kJ mol$^{-1}$.

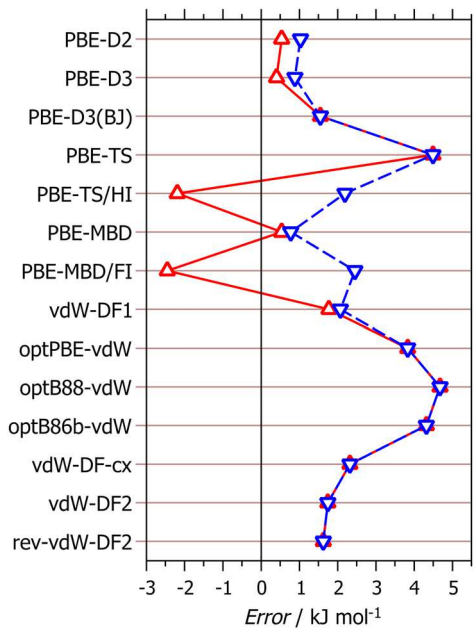


**FIG. 7**. MSE (red upright triangles) and MAE (blue inverse triangles) calculated from DFT energy differences $\Delta E_{DFT}$ and experimental enthalpies of transition $\Delta H_{trans}$.

- **MAE > 2 kJ mol$^{-1}$, MSE positive:** Functionals falling in this group exaggerate the relative instability of the less dense $SiO_2$ polymorphs. Here, vdW-DF1 and vdW-DF-cx still show a reasonable performance, with MAEs only slightly above 2 kJ mol$^{-1}$, whereas the errors of PBE-TS, optPBE-vdW, optB88-vdW, and optB86b-vdW are in the range of 4 to 5 kJ mol$^{-1}$.

Figure 8 shows a plot of all individual datapoints of $\Delta E_{DFT}$ against the framework density for PBE-D3, PBE-MDB, PBE-MDB/FI, optPBE-vdW, and rev-vdW-DF2 and compares them to the trendline based on experimental enthalpies of transition. It is evident that the trends identified above are fully confirmed by this approach: whereas datapoints obtained with the PBE-MBD/FI and optPBE-vdW functionals lie well below and above the trendline, respectively, those of the other three functionals fall much closer to it. Among these three, the rev-vdW-DF2 functional gives energy differences that are systematically too large, as one could deduce from the identical values of MSE and MAE (Fig. 7). For PBE-D3 and PBE-MBD, it is impossible to discern which of the two is more accurate on the basis of the available datapoints. In order to identify the "best" among the well-performing functionals, it would be necessary to perform a systematic study that includes a larger number of $SiO_2$-zeolites for which experimental enthalpies of transition are available. However, when considering the typical magnitude of experimental errors and the other assumptions that were made in the present work (especially the neglect of vibrational contributions), one might also argue that there is little point in making such fine distinctions. We may note that PBE-D3 calculations using the CP2K code[89] that were recently reported by one of us delivered an MAE of 1.4 kJ mol$^{-1}$ across a set containing $\alpha$-cristobalite and 16 all-silica zeolites, confirming the suitability of this functional to predict the relative stabilities of $SiO_2$ systems.[90]

Given the difficulties in performing calorimetric experiments to determine enthalpies of transition, one could also envisage a benchmarking of DFT against higher-level calculations, as is routinely done for molecular systems, where calculations using the coupled cluster method with single, double, and perturbative triple excitations [CCSD(T)] are often considered as "gold standard." However, performing such higher-level calculations is, at present, unfeasible for most periodic systems of interest. Nevertheless, we should mention that the energy difference between $\alpha$-quartz and $\alpha$-cristobalite was calculated by means of accurate quantum Monte Carlo (QMC) calculations by Hay *et al.*[12] Their QMC value of 1.9 ± 0.8 kJ mol$^{-1}$ compares well with the experimental enthalpy of transition of 2.8 kJ mol$^{-1}$.[86] For the quartz-cristobalite energy difference, nine of the 14 DFT-D and vdW-DF methods considered in the present work are also within 1 kJ mol$^{-1}$ of the experimental value. Clearly, further advancements in the development of highly accurate computational methods, especially their implementation for periodic solids, will facilitate the benchmarking of DFT methods.

An additional aspect that is worth commenting on is the qualitatively different behavior of the two TS-type approaches considered: where PBE-TS overestimates the energy differences and PBE-TS/HI underestimates them. It has been found before that the former functional overstabilizes the dense phases due to an exaggeration of dispersion interactions.[31] However, a replacement of conventional Hirshfeld partitioning by the iterative-Hirshfeld variant apparently leads to an overcorrection of this error. A similar issue is found when using the fractional-ion MBD method instead of PBE-MBD.

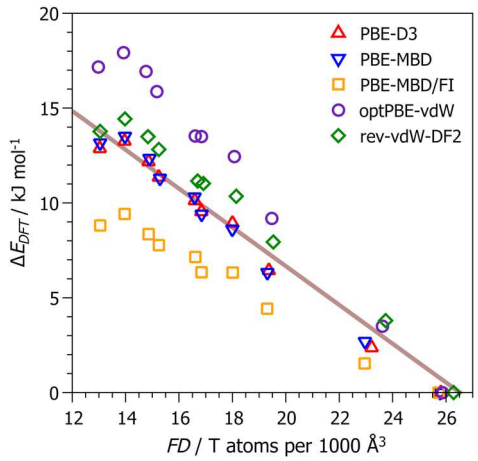


**FIG. 8**. Plot of the DFT energy difference $\Delta E_{DFT}$ against the framework density *FD* for selected functionals. The line corresponds to the experimental correlation between $\Delta H_{trans}$ and *FD* given in Eq. (5).

## D. Discussion

Altogether, we may summarize the performance of the different groups of approaches as follows:

- The tested GGA functionals without dispersion correction, PBE and PBEsol, perform very poorly for lattice parameters, bulk moduli, and relative stabilities, indicating that the inclusion of dispersion interactions is pivotal to correctly reproduce these quantities.
- An augmentation of the PBE functional with a Grimme-type dispersion correction affords a fairly accurate prediction of lattice parameters, bulk moduli, and relative stabilities. All three schemes appear to be quite robust, and the differences between them are rather intricate.
- The PBE-TS functional performs very well for lattice parameters but gives large errors in T–O–T angles, energetics, and bulk moduli. Use of the iterative-Hirshfeld variant PBE-TS/HI improves agreement with experiments in angles but worsens the prediction of lattice parameters.
- PBE-MBD does rather well for all structural parameters, gives relative stabilities of quantitative accuracy, and provides a reasonable prediction of bulk moduli. Altogether, it can be judged as the best approach if all quantities studied are considered to be equally relevant. Interestingly, use of the fractional-ion MBD approach deteriorates the performance for lattice parameters (slightly) and energetics (significantly).

- From the vdW-DF family of approaches, vdW-DF1 and vdW-DF2 give large deviations for lattice parameters, T–O bond lengths and bulk moduli, while providing a good prediction of the relative stabilities. The optPBE-vdW and—more markedly—optB88-vdW and optB86b-vdW functionals perform better for lattice parameters, but much worse for energetics and T–O–T angles. vdW-DF-cx and rev-vdW-DF2 show a more balanced performance across the board of quantities studied. Of the two, rev-vdW-DF2 can be considered to be the better choice due to the pronounced tendency of vdW-DF-cx to underestimate the T–O–T angles.

As already pointed out by Hay *et al.*,[12] error cancellation between overestimated T–O distances and underestimated T–O–T angles may lead to a good overall agreement in lattice parameters. This is indeed something we observe for several of the approaches considered, namely, the Grimme-type methods, the PBE-TS functional, as well as optPBE-vdW, optB88-vdW, and optB86b-vdW. The deterioration of the performance for lattice parameters when replacing PBE-TS by PBE-TS/HI can be attributed to precisely this phenomenon, as PBE-TS/HI gives more accurate (less underestimated) T–O–T angles and, consequently, too large lattice parameters. We have discussed above that the underestimation of T–O–T angles is likely caused by an overestimation of dispersion interactions between neighbouring T atoms. In this regard, it is worth noting that several of the functionals that suffer from this problem tend to overestimate bulk moduli and to overstabilise the dense phases, which is further evidence for a systematic overestimation of the role of dispersion interactions. On the other hand, the Grimme-type approaches underestimate the angles but give accurate relative stabilities, so one cannot straightforwardly extrapolate between different quantities and functionals.

## V. CONCLUSIONS

Altogether, we observe that several methods from both the DFT + D and the vdW-DF families deliver fairly accurate lattice parameters for neutral-framework zeotypes, with MAEs between 0.08 and 0.12 Å. However, we also have to note that many methods combine an overestimation of T–O bond distances with an underestimation of T–O–T angles, and good agreement for lattice parameters is, therefore, partly due to error cancellation. While the numerical values have to be treated with some caution due to the systematic difference between the DFT-optimized (0 K) structures and the experimental reference data, mostly obtained at room temperature, our previous work allows us to conclude that the observed deviations between DFT and experiments are considerably larger than the typical changes in lattice parameters between room temperature and cryogenic temperatures. In most instances, the methods that perform well for lattice parameters also give acceptable bulk moduli (PBE-TS is an exception). The reasonable agreement between DFT-computed and experimental bulk moduli for six of the seven compounds for which experimental values are available shows the robustness of the approach. However, we cannot, at present, elucidate the significant deviations for the seventh system, $ERI_{AlPO}$, which certainly warrants further attention from the side of computations.

With regard to relative stabilities, several methods that perform well for structural parameters significantly overestimate the energy difference between quartz and other phases (e.g., PBE-TS, optPBE-vdW, and optB88-vdW), i.e., they overstabilize the dense phase. Conversely, vdW-DF1 and vdW-DF2, which give significantly too large lattice parameters, do reasonably well for relative stabilities. Thus, these are indeed cases where we observe a "trade-off" between accuracy for structures and accuracy for energetics, as found in a previous benchmarking study for layered materials by Tawfik *et al.*[14] However, while only the PBE-MBD/FI functional and the *meta*-GGA SCAN-rVV10 functional were found to perform well for both interlayer distances and binding energies in the case of layered materials, there are actually several methods of varying complexity that provide good agreement for lattice parameters and relative stabilities for neutral-framework zeotypes. While PBE-MBD shows the best overall performance, rev-vdW-DF2 and some of the Grimme-type methods are also doing reasonably well, so all of these methods could be recommended, depending on the task in question: for example, PBE-D3 could be used in *ab initio* molecular dynamics studies for which PBE-MBD is too computationally demanding. At this point, we cannot elucidate the origin of the qualitatively different performance of some functionals for framework materials on the one hand, and layered materials on the other hand, but we hypothesize that the differences are related to the pronounced anisotropy of van der Waals interactions in the latter group of materials. Yet a different picture arises when looking at the binding energies of molecular complexes, for which different vdW-DF methods (vdW-DF2, rev-vdW-DF2, and, most prominently, vdW-DF-cx) outperform TS- and MBD-based dispersion-corrected approaches.[7] Altogether, it becomes more and more apparent that one cannot, at this point, expect general recommendations that would be valid across different groups of systems, as the choice of a suitable functional will depend both on the nature of the system in question and the quantity or quantities that are of most relevance. In the future, we will extend our investigations to adsorption enthalpies of guest molecules adsorbed in $SiO_2$ and $AlPO_4$ frameworks. In DFT studies of adsorption, the choice of an appropriate means to include dispersion interactions plays a pivotal role, as different approximate van der Waals methods may result in vastly different adsorption enthalpies, even for small molecules like methane or carbon dioxide.[20,23]

## SUPPLEMENTARY MATERIAL

See supplementary material for additional tables, including an EXCEL sheet reporting the individual results, and DFT-optimized structures in CIF format.

## ACKNOWLEDGMENTS

The authors acknowledge Torbjörn Björkman for making his implementation of the vdW-DF-cx functional in VASP

available to them. M.F. acknowledges funding by the Deutsche Forschungsgemeinschaft (DFG, German Research Foundation), Project No. 389577027 (FI1800/5-1). A research visit of M.F. to Nancy that initiated this collaboration was funded by the Central Research Development Funds of the University of Bremen. Part of the calculations were conducted using GENCI-CCRT/CINES computational resources under Grant No. x2018-A0040910433.

## REFERENCES

[1] A. M. Reilly and A. Tkatchenko, Chem. Sci. **6**, 3289 (2015).
[2] S. Grimme, A. Hansen, J. G. Brandenburg, and C. Bannwarth, Chem. Rev. **116**, 5105 (2016).
[3] J. Hermann, R. A. DiStasio, and A. Tkatchenko, Chem. Rev. **117**, 4714 (2017).
[4] R. Sedlak, T. Janowski, M. Pitoňák, J. Rezáč, P. Pulay, and P. Hobza, J. Chem. Theory Comput. **9**, 3364 (2013).
[5] J. Rezáč and P. Hobza, Chem. Rev. **116**, 5038 (2016).
[6] K. Remya and C. H. Suresh, J. Comput. Chem. **34**, 1341 (2013).
[7] J. Claudot, W. J. Kim, A. Dixit, H. Kim, T. Gould, D. Rocca, and S. Lebègue, J. Chem. Phys. **148**, 064112 (2018).
[8] J. Binns, M. R. Healy, S. Parsons, and C. A. Morrison, Acta Crystallogr., Sect. B: Struct. Sci., Cryst. Eng. Mater. **70**, 259 (2014).
[9] D. J. Carter and A. L. Rohl, J. Chem. Theory Comput. **10**, 3423 (2014).
[10] T. Björkman, A. Gulans, A. V. Krasheninnikov, and R. M. Nieminen, J. Phys.: Condens. Matter **24**, 424218 (2012).
[11] D. Tunega, T. Bučko, and A. Zaoui, J. Chem. Phys. **137**, 114105 (2012).
[12] H. Hay, G. Ferlat, M. Casula, A. P. Seitsonen, and F. Mauri, Phys. Rev. B **92**, 144111 (2015).
[13] F. Tran, J. Stelzl, and P. Blaha, J. Chem. Phys. **144**, 204120 (2016).
[14] S. A. Tawfik, T. Gould, C. Stampfl, and M. J. Ford, Phys. Rev. Mater. **2**, 034005 (2018).
[15] T. Gould, S. Lebègue, J. G. Ángyán, and T. Bučko, J. Chem. Theory Comput. **12**, 5920 (2016).
[16] W. Vermeiren and J.-P. Gilson, Top. Catal. **52**, 1131 (2009).
[17] S. Kulprathipanja, in *Zeolites in Industrial Separation and Catalysis*, edited by S. Kulprathipanja (Wiley-VCH Verlag GmbH & Co. KGaA, Weinheim, Germany, 2010).
[18] A. F. Masters and T. Maschmeyer, Microporous Mesoporous Mater. **142**, 423 (2011).
[19] V. Van Speybroeck, K. Hemelsoet, L. Joos, M. Waroquier, R. G. Bell, and C. R. A. Catlow, Chem. Soc. Rev. **44**, 7044 (2015).
[20] F. Göltl, A. Grüneis, T. Bučko, and J. Hafner, J. Chem. Phys. **137**, 114111 (2012).
[21] H. Fang, P. Kamakoti, J. Zang, S. Cundy, C. Paur, P. I. Ravikovitch, and D. S. Sholl, J. Phys. Chem. C **116**, 10692 (2012).
[22] M. Fischer and R. G. Bell, Z. Kristallogr. - Cryst. Mater. **228**, 124 (2013).
[23] J. Shang, G. Li, R. Singh, P. Xiao, D. Danaci, J. Z. Liu, and P. A. Webley, J. Chem. Phys. **140**, 084705 (2014).
[24] M. Fischer, M. Rodríguez Delgado, C. Otero Areán, and C. Oliver Duran, Theor. Chem. Acc. **134**, 91 (2015).
[25] S. Chibani, M. Chebbi, S. Lebègue, T. Bučko, and M. Badawi, J. Chem. Phys. **144**, 244705 (2016).
[26] E. P. Hessou, W. G. Kanhounnon, D. Rocca, H. Monnier, C. Vallières, S. Lebègue, and M. Badawi, Theor. Chem. Acc. **137**, 161 (2018).
[27] B. Civalleri, C. M. Zicovich-Wilson, P. Ugliengo, V. R. Saunders, and R. Dovesi, Chem. Phys. Lett. **292**, 394 (1998).
[28] R. Astala, S. M. Auerbach, and P. A. Monson, J. Phys. Chem. B **108**, 9208 (2004).
[29] M. A. Zwijnenburg, F. Corá, and R. G. Bell, J. Phys. Chem. B **111**, 6156 (2007).
[30] E. I. Román-Román and C. M. Zicovich-Wilson, Chem. Phys. Lett. **619**, 109 (2015).
[31] M. Fischer, F. O. Evers, F. Formalik, and A. Olejniczak, Theor. Chem. Acc. **135**, 257 (2016).
[32] M. Fischer and R. J. Angel, J. Chem. Phys. **146**, 174111 (2017).
[33] A. Albavera-Mata, C. M. Zicovich-Wilson, J. L. Gázquez, S. B. Trickey, and A. Vela, Theor. Chem. Acc. **137**, 26 (2018).
[34] M. Dion, H. Rydberg, E. Schroder, D. C. Langreth, and B. I. Lundqvist, Phys. Rev. Lett. **92**, 246401 (2004).
[35] J. P. Perdew, K. Burke, and M. Ernzerhof, Phys. Rev. Lett. **77**, 3865 (1996).
[36] H. Rydberg, M. Dion, N. Jacobson, E. Schroder, P. Hyldgaard, S. I. Simak, D. C. Langreth, and B. I. Lundqvist, Phys. Rev. Lett. **91**, 126402 (2003).
[37] K. Lee, E. D. Murray, L. Kong, B. I. Lundqvist, and D. C. Langreth, Phys. Rev. B **82**, 081101 (2010).
[38] J. P. Perdew and Y. Wang, Phys. Rev. B **33**, 8800(R) (1986).
[39] J. Kilmeš, D. Bowler, and A. Michaelides, J. Phys.: Condens. Matter **22**, 022201 (2010).
[40] J. Klimeš, D. R. Bowler, and A. Michaelides, Phys. Rev. B **83**, 195131 (2011).
[41] K. Berland and P. Hyldgaard, Phys. Rev. B **89**, 035412 (2014).
[42] A. D. Becke, J. Chem. Phys. **85**, 7184 (1986).
[43] I. Hamada, Phys. Rev. B **89**, 121103 (2014).
[44] S. Grimme, J. Comput. Chem. **27**, 1787 (2006).
[45] S. Grimme, J. Antony, S. Ehrlich, and H. Krieg, J. Chem. Phys. **132**, 154104 (2010).
[46] S. Grimme, S. Ehrlich, and L. Goerigk, J. Comput. Chem. **32**, 1456 (2011).
[47] A. Tkatchenko and M. Scheffler, Phys. Rev. Lett. **102**, 073005 (2009).
[48] P. Bultinck, C. Van Alsenoy, P. W. Ayers, and R. Carbó Dorca, J. Chem. Phys. **126**, 144111 (2007).
[49] T. Bučko, S. Lebègue, J. Hafner, and J. G. Ángyán, J. Chem. Theory Comput. **9**, 4293 (2013).
[50] A. Tkatchenko, R. A. Di Stasio, R. Car, and M. Scheffler, Phys. Rev. Lett. **108**, 236402 (2012).
[51] R. A. DiStasio, Jr., O. A. von Lilienfeld, and T. Tkatchenko, Proc. Natl. Acad. Sci. U. S. A. **109**, 14791 (2012).
[52] A. Ambrosetti, A. M. Reilly, R. A. DiStasio, Jr., and T. Tkatchenko, J. Chem. Phys. **140**, 18A508 (2014).
[53] T. Gould and T. Bučko, J. Chem. Theory Comput. **12**, 3603 (2016).
[54] G. Kresse and J. Hafner, Phys. Rev. B **48**, 13115 (1993).
[55] G. Kresse and J. Furthmüller, Phys. Rev. B **54**, 11169 (1996).
[56] P. Vinet, J. Ferrante, J. H. Rose, and J. R. Smith, J. Geophys. Res. **92**, 9319, https://doi.org/10.1029/jb092ib09p09319 (1987).
[57] T. Bučko, S. Lebègue, J. Hafner, and J. G. Ángyán, Phys. Rev. B **87**, 064110 (2013).
[58] T. Bučko, S. Lebègue, T. Gould, and J. G. Ángyán, J. Phys.: Condens. Matter **28**, 045201 (2016).
[59] G. Román-Pérez and J. M. Soler, Phys. Rev. Lett. **103**, 096102 (2009).
[60] T. Björkman, J. Chem. Phys. **141**, 074708 (2014).
[61] C. Baerlocher and L. McCusker, Database of Zeolite Structures, http://www.iza-structure.org/databases, 2018.
[62] K. Kihara, Eur. J. Miner. **2**, 63 (1990).
[63] J. J. Pluth, J. V. Smith, and J. Faber, J. Appl. Phys. **57**, 1045 (1985).
[64] M.-J. Díaz-Cabañas, P. A. Barrett, and M. A. Camblor, Chem. Commun. **1998**, 1881.
[65] J. A. Hriljac, M. M. Eddy, A. K. Cheetham, J. A. Donohue, and G. J. Ray, J. Solid State Chem. **106**, 66 (1993).
[66] J. E. Lewis, C. C. Freyhardt, and M. E. Davis, J. Phys. Chem. **100**, 5039 (1996).
[67] L. A. Villaescusa, P. Lightfoot, S. J. Teat, and R. E. Morris, J. Am. Chem. Soc. **123**, 5453 (2001).
[68] A. Corma, F. Rey, J. Rius, M. J. Sabater, and S. Valencia, Nature **431**, 287 (2004).
[69] B. Marler, A. Grünewald-Lüke, and H. Gies, Microporous Mesoporous Mater. **26**, 49 (1998).

[70]D. S. Wragg, R. Morris, A. W. Burton, S. I. Zones, K. Ong, and G. Lee, Chem. Mater. **19**, 3924 (2007).
[71]J. J. Williams, Z. A. D. Lethbridge, G. J. Clarkson, S. E. Ashbrook, K. E. Evans, and R. I. Walton, Microporous Mesoporous Mater. **119**, 259 (2009).
[72]B. P. Onac and H. S. Effenberger, Am. Miner. **92**, 1998 (2007).
[73]H. A. Graetsch, Neues Jahrb. Mineral., Monatsh. **2003**, 289.
[74]R. M. Kirchner, R. W. Grosse-Kunstleve, J. J. Pluth, S. T. Wilson, R. W. Broach, and J. V. Smith, Microporous Mesoporous Mater. **39**, 319 (2000).
[75]M. Amri and R. I. Walton, Chem. Mater. **21**, 3380 (2009).
[76]M. P. Attfield and A. W. Sleight, Chem. Mater. **10**, 2013 (1998).
[77]M. Afeworki, D. L. Dorset, G. J. Kennedy, and K. G. Strohmaier, Chem. Mater. **18**, 1697 (2006).
[78]L. Levien, C. T. Prewitt, and D. J. Weidner, Am. Miner. **65**, 920 (1980).
[79]A. Yeganeh-Haeri, D. J. Weidner, and J. B. Parise, Science **257**, 650 (1992).
[80]H. Sowa, J. Macavei, and H. Schulz, Z. Kristallogr. **192**, 119 (1990).
[81]M. Colligan, P. M. Forster, A. K. Cheetham, Y. Lee, T. Vogt, and J. A. Hriljac, J. Am. Chem. Soc. **126**, 12015 (2004).
[82]P. Lotti, R. Arletti, G. D. Gatta, S. Quartieri, G. Vezzalini, M. Merlini, V. Dmitriev, and M. Hanfland, Microporous Mesoporous Mater. **218**, 42 (2015).
[83]J.-M. Thibaud, J. Rouquette, P. Hermet, K. Dziubek, F. A. Gorelli, M. Santoro, G. Garbarino, F. G. Alabarse, O. Cambon, F. Di Renzo, A. van der Lee, and J. Haines, J. Phys. Chem. C **121**, 4283 (2017).
[84]F. G. Alabarse, G. Silly, J.-B. Brubach, P. Roy, A. Haidoux, C. Levelut, J.-L. Bantignies, S. Kohara, S. Le Floch, O. Cambon, and J. Haines, J. Phys. Chem. C **121**, 6852 (2017).
[85]P. M. Piccione, C. Laberty, S. Yang, M. A. Camblor, A. Navrotsky, and M. E. Davis, J. Phys. Chem. B **104**, 10001 (2000).
[86]A. Navrotsky, O. Trofymluk, and A. A. Levchenko, Chem. Rev. **109**, 3885 (2009).
[87]R. T. Downs, G. V. Gibbs, K. L. Bartelmehs, and M. B. Boisen, Am. Miner. **77**, 751 (1992).
[88]M. Fischer, "Template effects on the pressure-dependent behavior of chabazite-type fluoroaluminophosphates: a computational approach," Phys. Chem. Miner. (to be published).
[89]J. Hutter, M. Iannuzzi, F. Schiffmann, and J. VandeVondele, Wiley Interdiscip. Rev.: Comput. Mol. Sci. **4**, 15 (2014).
[90]M. Fischer, J. Phys. Chem. C **123**, 1852 (2019).